

Thermal Analysis of MCM Packaging

A. Andonova¹

¹*Department of Microelectronics, Technical University of Sofia,
Kiment Ohridski St. 8, BG-1797 Sofia, Bulgaria
ava@ecad.tu-sofia.bg*

Abstract—This paper describes the use of infra-red thermography for the thermal study in the development stage of custom enclosures for multi-chip modules. Some limitations of conventional thermographic measurements are discussed and an approach for enhancing its application to quality control and diagnostics of faulty multi-chip module packages is proposed. The results from thermal measurements of radio-frequency range multi-chip module prototype in an open and a closed Quad Flat No Lead package are presented.

Index Terms—Electronic packaging thermal management, Infrared thermography, Multichip modules, Thermal analysis

I. INTRODUCTION

Thermal problems of the modern packaging methods pose a huge challenge in making decisions during thermal design process [1].

The use of new solutions in packaging is linked to amendment and improvement of technology processes. So new mechanisms of failures can arise and it is therefore necessary to develop diagnostic techniques and to introduce new criteria for assessing the reliability which are directly related to thermal phenomena in microelectronic devices.

Some of the typical representatives of modern packaging methods are the Multi-Chip Modules (MCMs).

With higher chip densities, the thermal management of MCMs poses a challenge to package manufacturing. The complexity of the problem and the nature of the solution techniques have created high degree of uncertainty in the results. From the failure perspective the temperature is active factor for most failure models, so temperature reduction will significantly improve the expected reliability of MCMs [2]. High operating temperatures can also reduce the RF (radio-frequency range) MCM performance [3], [4].

Packaging of RF MCM has traditionally been very expensive. The requirements for packaging are extremely demanding: very high electrical isolation and excellent signal integrity to high frequencies as well as the ability to accommodate GaAs ICs dissipating significant amounts of heat.

The packages of Quad Flat No Leads (QFN) type respond to the consumer demand for more functional packages with small size and compact structure.

Advanced Infra-Red Thermography (IRT) systems scan and visualize fast transient temperature processes. Thus,

remote nondestructive monitoring is done and evaluation of the parameters of real transient thermal processes in MCM is carried out. Surface temperature measurement provides useful information when to do diagnosis, monitoring of operation processes or degradation processes, and when to do fault detection [5].

Recently, more researchers employ thermal simulations [6] and thermal measurements [7], which give promising results and significantly shorten the cost and time-to-market. Reported results for the implementation of such approach for RF MCM are almost missing in scientific publications.

There are two aspects of the thermal performance of assembled and mounted MMIC (Monolithic Microwave Integrated Circuit) package: one, the plated metals on the bottom side of the package that is MMIC mounting area, RF ground and low thermal resistance connection, and two, the motherboard mounting area [8].

The aim of this paper is to show the advantages of IRT in studying heat removal from the QFN packaging prototypes of specialized RF MCM. Experimental data that needs to be accountable for the successful implementation of QFN technology in the process of RF MCM assembly is reviewed and analysed. The results of the RF MCM study for the needs of mobile satellite telecommunications are used to demonstrate the proposed methodology.

II. RF MCM WITH QFN PACKAGE

The subject of present study is a prototype of a specialized RF MCM, including analogue GaAs chip and standard CMOS chip of shift registers to control electronic switches. Generally, the module has mixed analog-to-digital functions and controls the antenna element of a phased array antenna. The developed device is an exclusive proprietary patent and know-how of RaySat company, so that detailed data about its parameters will not be presented.

The main GaAs chip that is the heart of the developed MCM is manufactured using pHEMT technology and is designed to operate in the frequency range of 10-14 GHz.

The module includes:

- Three bare chips of CMOS shift registers for implementing serial-to-parallel interface;
- One bare GaAs chip for basic functions;
- Connection between chips and the input/output pin pads by bonding wires.

A package QFN type with dimensions $7 \times 7 \times 1$ mm is used. It is shown in Fig. 1.

The material of the packaging is sheet ceramics – three

Manuscript received November 27, 2013; accepted January 8, 2014.

This research was funded by a grant (No. DFNI-I01/9-3) from the National Ministry of Science and Education of Bulgaria.

layer structure with three levels of metallization and technology for the preparation of the packaging – LTCC (Low Temperature Co-fired Ceramic).

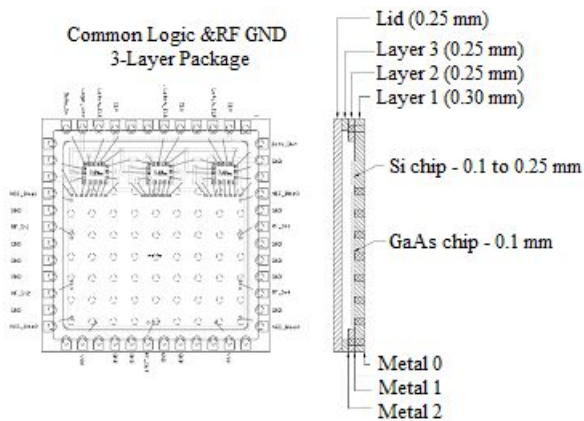


Fig. 1. Layout picture of microwave ceramic packages (courtesy of Ray Sat BG Ltd).

Thermal IRT measurements are performed in an open and a closed package in two modes, as the temperature difference of 2 °C between the two states is reported.

The common figure-of-merit that is usually used for comparison of various thermal designs is the junction-to-ambient thermal resistance, j_a . However, this single parameter cannot effectively describe the three dimensional heat flows in multi-chip modules. The temperature difference between the heat sources and the case in a multi-chip module is radically affected by the heat dissipation from the neighbouring components, the heat paths within the module, and the cooling conditions [9].

This fact must be taken into consideration regarding the obtained results which have rather relative character because the influence of the other elements of the PCB is not reported. For reducing the error between the simulated and the experimental data a test fixture with a single QFN carrier is designed. The test fixture is shown in Fig. 2(a) and the back side of the module carrier respectively is shown in Fig. 2(b). 3D micro-contact elements pin-ring type [10] for the process of mounting of QFN carrier to the PCB are developed for assembly and disassembly of the carrier to the PCB (especially in testing), as shown in Fig. 2(c).

There was realized the idea of mounting the MCM without heat treatment as well as the easy substitution of the defected chip by using both micro-contact elements: a stud over the chip-carrier and a ring over the substrate-carrier [11].

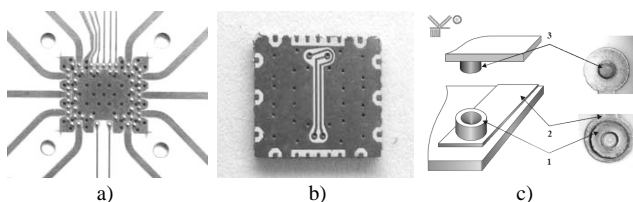


Fig. 2. Pictures of: (a) a test fixture; (b) a back side of the chip carrier; (c) 3D micro-components from pin-ring type [11].

In Fig. 3(a) a 3D compact CFD generalized model is shown with enclosure, using a network of $36 \times 26 \times 34$ cells. One of the advantages of using CFD (FLOTHERM

software) is that the local thermal conductivity of the package and the PCB are calculated by the program. Figure 3(b) shows the temperature profile of the QFN package mounted on PCB at an ambient temperature of 25 °C.

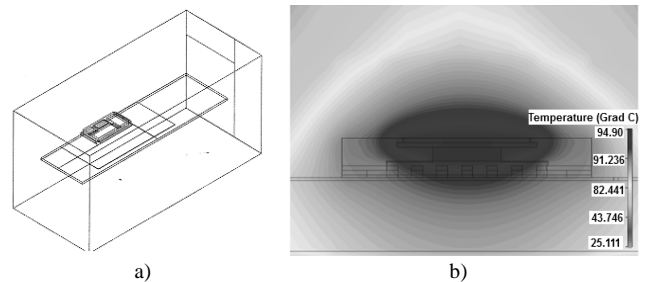


Fig. 3. Results from CFD simulation: (a) 3D compact model; (b) temperature profile of a QFN package.

The distribution of the heat flow from the QFN packaging for power of 1W is the following:

- Top of the package: 194.6 mW (89.4 mW convection, 105.2 mW radiation);
- Base of the package: 159.6 mW (at the board);
- Walls of the package: 18 mW (convection);
- Conclusions: 627.8 mW (38 mW losses in the air, the rest is in the pins in the package);
- Total flow entering the package: 749.4 mW.

It has been proven that the circuit board acts as a cooling radiator with 75 % of the dissipated power enters through the air openings of the circuit board which are disposed under the MCM carrier. Power dissipation and boundary conditions for the ambient temperature (21.5 °C) in the CFD model are well consistent with the experimental measurements. The estimated value of the thermal resistance “junction-ambient” is 36.1 °C/W, and the measured temperature is 37.5 °C/W.

III. EXPERIMENTAL SETUP

IRT is a convenient method for 2D contactless measurement of surface temperatures. The data of the temperature field in the form of thermogram or sequence of thermograms can be used to obtain information about thermal phenomena which occur during the operation. The vision system elaborated within the framework of the research described in this work is intended for MCM testing during the packaging process and for diagnosis of failures in MMIC for QFN package (if needed).

The IRT system includes hardware and software parts. The hardware part consists of a camera and a portable PC to record in real time. The main task of this part is to observe the MCM surface by means of infra-red camera. The device used is a FLIR ThermaCAM SC640 imaging system. It has a 640×420 pixels focal-plane-array uncooled micro-bolometer detector, with a sensitive range of 7.5 μm -13 μm and close-up lens. Imaging and storage is made at a frequency rate of 50 Hz. The thermal sensitivity of the camera is 0.08 °C at 30 °C. The PC is equipped with ThermaCam Researcher 2.9 software; this software is used to analyse dynamic infra-red radiation records in real time, including the emissivity calculations.

IV. RESULTS AND ANALYSIS

One big source of error in temperature measurements of s with an infrared camera is the emissivity variation over their surface. These devices are constructed from materials with widely ranging emissivity values – below 0.1 for gold and other unoxidised metals to near unity for ceramics.

The voltage output signal of the FPA detector, $V(T)$, is proportional to Plank's law and can be written as

$$V(t) = \int_{\lambda_1}^{\lambda_2} \frac{k(\lambda)v(\lambda)}{\lambda^5 [\exp(c_2/\lambda T) - 1]} d\lambda, \quad (1)$$

on the following assumptions: $k(\lambda) = k$ (the detector properties are independent of the wavelength) and $v(\lambda) = \epsilon$ (the object is a grey body), where k is a union of constant of the detector and Plank's law, $[\lambda_1, \lambda_2]$ is the spectral range of the detector and $c_2 = hc_0/k = 1.439 \times 10^4 \mu\text{mK}$. Since all materials have different dependencies of $v(\lambda)$ and this consideration applies to an arbitrary material the material is assumed to be grey body, i.e. $v(\lambda) = \epsilon$. Another assumption is that the detector properties are independent of the wavelength, i.e. $k(\lambda) = k$. From these assumptions it can be written

$$V(t) = kV \int_{\lambda_1}^{\lambda_2} \frac{d\lambda}{\lambda^5 [\exp(c_2/\lambda T) - 1]} = kV F_{12}(T). \quad (2)$$

This equation can be used to yield an expression for the temperature error caused by an uncertainty of emission. An assumed emissivity ϵ_m results in a measured temperature T_m . The signal that yields T_m is the same signal $V(T)$, that would yield the correct temperature T if the correct emissivity ϵ was assumed.

Two approaches are used for emissivity effect compensation. The first one is based on emissivity correction. It uses actual measurements of the effective emissivity distribution of the MMIC. By using a hot plate (Titanium hot plate PZ 28-3 TPD with programmable controller PR5 3T for precise temperature regulation) the unpowered MCM is heated to two known temperatures T_1 and T_2 ($T_2 - T_1 > 20 \text{ }^\circ\text{C}$) in sequence. A radiance image is recorded at each temperature. The emissivity matrix is computed and stored when the temperature and radiance for two temperatures are known. This matrix is subsequently used for correcting the power radiance image of MCM device and a true temperature thermogram can be provided.

The second approach lies in applying a coating layer to a certain value of the emissivity which is close to 1 on the surface of the electronic device [12]. To offset the effects of surface emissivity a specially prepared solution of glycerine ($\epsilon = 0.98$) is used. Measurements have shown that in this way the measured surface temperature is about $2 \text{ }^\circ\text{C}$ lower than the temperature of the closed QFN package. This approach can be used when performing IRT thermal analysis of MCM prototypes or detecting the failures of MCM with open QFN package. Figure 4(a) and Fig. 4(b) shows thermograms at different loading of MCM, in which only the

left CMOS IC and the majority of the surface of the GaAs IC in the unclosed QFN package are coated with glycerine solution.

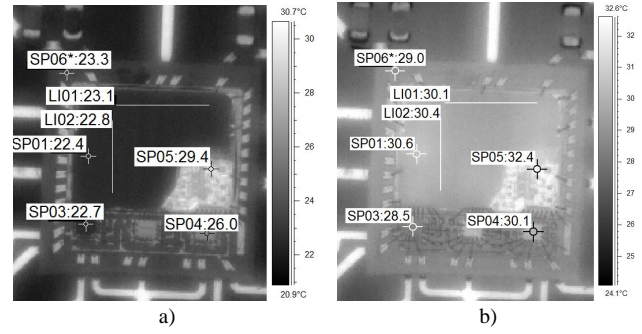


Fig. 4. Thermograms of (a) unloaded and (b) loaded RF MCM in unclosed QFN package, with a partially covered surface with glycerine solution.

These thermograms are processed by ThermaCam Researcher software and they show the measured temperatures (which may be max/min/average) in the marked spots and lines. When corrections of atmospheric and reflected temperatures, distance, relative humidity and object emissivity are made, the temperature field on the MCM surface can be monitored in real-time.

Figure 5 shows successive thermograms of the MCM from left to right – before and after switching on the load, and a thermogram is synthesized where each pixel constitutes the temperature difference of the corresponding pixels in the two images. This is the case in which the relative change of the heat distribution may be qualitatively evaluated. In this case, correction of the emissivity is not made. Thus, the change of heat transfer from the QFN package to the PCB can be seen on-line.

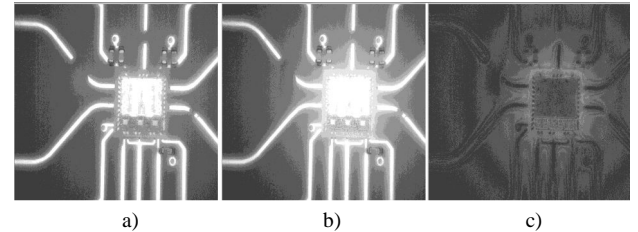


Fig. 5. Thermograms (from left to right direction) before and after switching on the load and a synthesised thermogram.

To extract useful information during the thermal diagnosis of MCM a proper filtration for the purposes is proposed. When we want to accurately locate the temperature field Laplacian of Gaussian (LoG) filter can be used. The expression for the two-dimensional (2-D) LoG function located in the centre of the coordinate system and using Gaussian distribution with standard deviation σ has the form

$$\text{LoG}(x, y) = -\frac{1}{f\sigma^4} \left(1 - \frac{x^2 + y^2}{2\sigma^2} \right) e^{-\frac{x^2 + y^2}{2\sigma^2}}. \quad (3)$$

Both Gaussian (noise reduction) and Laplace (edge detection) filters are applied by performing an operation convolution of the image with a matrix of numbers. In the essence, the effect of this filter is to outline the contours of the objects in the image. LoG operator calculates the second

derivative of the image intensity and is isotropic. In Fig. 6(a) the row thermogram and Fig. 6(b) the result after LoG filtering are shown.

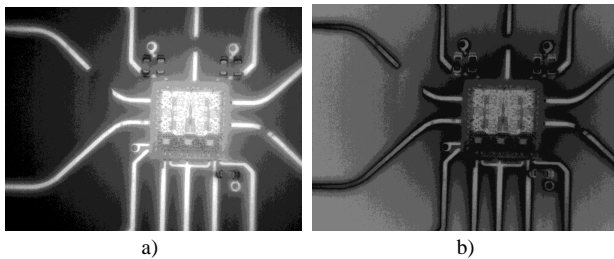


Fig. 6. Row thermogram and (a), LoG filtered image of RF MCM in an uncovered QFN package (b).

In order to improve the contrast in the image normalization may be carried out. Figure 7 shows the histograms of the normalized images in Fig. 6. One can distinguish the differences between histograms of row infrared image and the filtered image. The histograms, which are also available in real time, can be used for evaluation of the temperature field of the MCM.

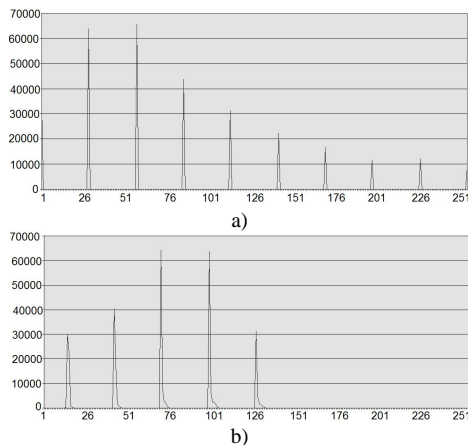


Fig. 7. Histograms of the row infrared image (a) and the filtered image (b) respectively in Fig 6.

The IRT system makes an infrared image that allows it to check the MCM for possible defects. These are shown as hot spots/areas in the image, resulting from the higher surface temperature of a faulty device. In the quality control process, each MCM is loaded for a very short period of time. The thermal imaging camera observes the thermal cycle of the device. The computer compares the maximum detected temperature with the average surface temperature of the tested MCM. If the difference between the maximum and average values exceeds a predefined value, this means that the MCM has a hot spot/area.

In the Fig. 8 thermograms of MCMs are shown with and without potential defect of GaAs IC. The first two thermograms are for MCMs in the same mode of operation. On the left, the image of defective MMIC is shown, in the middle stays the image of the nondefective (reference) MMIC and the third thermogram is the result of the subtraction of the first two pixel by pixel.

The measurement is made for an open QFN package. On the thermogram which is a result from subtraction there a localized hotter region is observed. This indicates a potential defect.

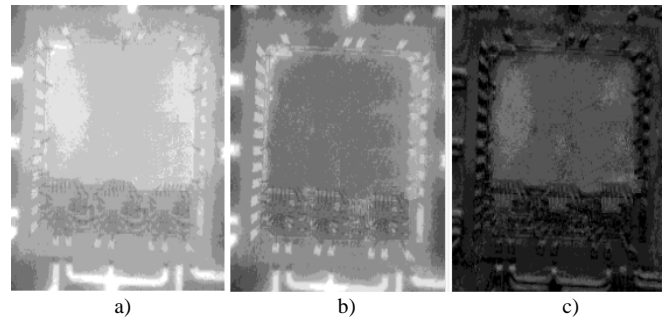


Fig. 8. Thermograms of the loaded a defective and an etalon MCM modules and the subtraction thermogram (from left to right).

V. CONCLUSIONS

The presented paper shows how an examination of the temperature distribution of the prototypes of packaged and unpackaged MCMs can be performed for thermal management purposes by using IRT system. Passive and active (step heating and pulse) thermography can be applied in quality control and for detection of defects in MSMs. The application of nondestructive IRT with or without thermocouples and thermal simulations leads to shortening the development time of custom MCM packages with respect to improving their thermal robustness and leads to significant reduction of the cost for their quality.

REFERENCES

- [1] AN 0018 *United Monolithic Semiconductors S.A.S.*, France, 2009. Online [Available]: http://www.ums-gaas.com/telechargement/AN0018_9084_Thermal_Management_for_Dies_and_Packages_1.pdf
- [2] A. Christou, W. Webb, *GaAs MMIC Reliability - High Temperature Behavior*. RIAC, 2006.
- [3] C. H. Oxley, B. M. Coaker, N. E. Priestley, "Measured thermal images of a gallium arsenide power MMIC with and without RF applied to the input", *Solid-State Electronics*, vol. 47, no. 4, pp. 755–758, 2003. [Online]. Available: [http://dx.doi.org/10.1016/S0038-1101\(02\)00356-8](http://dx.doi.org/10.1016/S0038-1101(02)00356-8)
- [4] R. Hopper, D. Prime, G. Evans, K. Lee, C. Oxley, "Improved infrared temperature measurement of RF devices", 2013. [Online] Available: <http://www.armms.org/media/uploads/1326110849.pdf>
- [5] Ch. Schmidt, F. Altmanna, O. Breitenstein, "Application of lock-in thermography for failure analysis in integrated circuits using quantitative phase shift analysis", *Materials Science and Engineering*, vol. B 177, pp. 1261–1267, 2012.
- [6] B. Xu, H. Li, "Thermal design, analysis and verification of chip-level MCM with properties of semiconductor materials", *Advanced Materials Research*, vol. 625, pp. 280–286, 2012. [Online]. Available: <http://dx.doi.org/10.4028/www.scientific.net/AMR.625.280>
- [7] F. Xunlei, Y. Wei, J. Weizhuo, "Application to three-dimensional microwave module using infrared thermography", *AISM*, Xijian, China, pp. 825–829, 2004.
- [8] S. Melvin, "Custom MMIC packaging solutions for high frequency thermally efficient surface mount applications". [Online] Available: <http://www.armms.org/media/uploads/1335467588.pdf>
- [9] B. Lall, B. Guenin, "Methodology for thermal evaluation of multichip modules", *IEEE Trans. CPMT-PART A*, vol. 18, no. 4, pp. 758–764, 1995.
- [10] S. Andreev, R. Arnaudov, A. Andonova, N. Kafadarova, V. Videkov, "Development and investigation of horizontal elements in 3D micro-contacts and structures", *ESTC*, Greenwich, UK, 2008, pp. 1285–1289.
- [11] R. Arnaudov, A. Andonova, N. Kafadarova, S. Andreev, V. Videkov, "Experimental characterization of 3D micro-contacts", *ISSE*, Budapest, Hungary, 2008, pp. 535–539.
- [12] M. Gradhand, O. Breitenstein, "Preparation of nonconducting infrared-absorbing thin films", *Review of Scientific Instruments*, vol. 76, no. 5, pp. 53702, 2005. [Online]. Available: <http://dx.doi.org/10.1063/1.1896620>